

## Critical exponents with a multiscale entanglement renormalization Ansatz channel

S. Montangero,<sup>1,2</sup> M. Rizzi,<sup>3</sup> V. Giovannetti,<sup>2</sup> and Rosario Fazio<sup>2</sup>

<sup>1</sup>*Institut für Quanteninformationsverarbeitung, Universität Ulm, D-89069 Ulm, Germany*

<sup>2</sup>*NEST CNR-INFN and Scuola Normale Superiore, Piazza dei Cavalieri 7, I-56126 Pisa, Italy*

<sup>3</sup>*Max-Planck-Institut für Quantenoptik, Hans-Kopfermann-Str. 1, D-85748 Garching, Germany*

(Received 11 December 2008; revised manuscript received 23 June 2009; published 30 September 2009)

We show how to compute the critical exponents of one-dimensional quantum critical systems in the thermodynamic limit. The method is based on an iterative scheme applied to the multiscale entanglement renormalization Ansatz for the ground-state wave function. We test this scheme to compute the critical exponents of the Ising and XXZ model for which we can compare the method with the exact values. The agreement is at worst within few percent of the exact results already for moderate dimensions of the tensor indices.

DOI: [10.1103/PhysRevB.80.113103](https://doi.org/10.1103/PhysRevB.80.113103)

PACS number(s): 64.70.Tg, 03.67.-a, 05.30.-d, 89.70.-a

Finding accurate methods for computing critical behavior has been central to physics since the development of renormalization group. Critical phenomena are ubiquitous in nature ranging from condensed-matter systems to biological systems or even economic systems. A key concept in their description is that of scale invariance,<sup>1</sup> i.e., the existence of diverging correlation lengths which manifest in power-law decays of the system correlation functions. Characterizing the physics of these complex phenomena requires thus to compute either analytically or numerically the *critical exponents* of the system,<sup>2</sup> i.e., the exponents which govern such power-law decays.

In recent years several proposals<sup>3-5</sup> have been put forward to address this problem by proposing generalizations of the density-matrix renormalization group (DMRG) approach<sup>6</sup> for efficiently representing the ground-state properties of critical Hamiltonians. Among these attempts the multiscale entanglement renormalization Ansatz (MERA) introduced by Vidal<sup>5</sup> is particularly appealing. Similarly to DMRG it can be casted in a variational Ansatz in terms of a special class of many-body quantum states. However in DMRG such class (i.e., the matrix product states<sup>6-11</sup>) lacks of the fundamental ingredient (i.e., scale invariance) for efficiently reproducing the physics of a system at criticality. On the contrary in MERA the class consists in a collection of states (the MERA states) which have an intrinsic scale-invariance structure built in.

A method for computing the critical exponents associated with a given MERA state has been very recently put forward by some of us<sup>12</sup> by relating them to the eigenvalues of the MERA transfer matrix. In the present work we briefly review the MERA tensor-network formalism and this method. Building up from such results we then introduce a numerical algorithm for finding the optimal MERA state which best approximates the ground state of a critical, translationally invariant Hamiltonian. This is the main result of this Brief Report. As a test of its efficiency we apply such an algorithm for studying the critical exponents of two cornerstone models in quantum statistical mechanics, the Ising and the XXZ model. In one dimension the critical exponents of these models are exactly known, thus providing a highly nontrivial case where to see the method<sup>12</sup> at work.

Consider a one-dimensional translational invariant many-body quantum system at criticality composed of  $L=2^\ell$  sites (each site being  $m$  dimensional), characterized by a local

Hamiltonian  $H$  which involves at most next-nearest-neighboring interaction terms (generalization to longer-but-finite range interactions is straightforward, by considering the far away operators as neighbors after a certain number of renormalizations<sup>5</sup>). Under these conditions we can write  $H=\sum_{k=1}^L h_k$  with  $h_k$  acting on the triple composed by the three consecutive sites  $k-1$ ,  $k$ , and  $k+1$  of the system where we identify the  $(L+1)$ th and the zeroth sites with the 1th and the  $L$ th sites, respectively, to enforce the proper periodic boundary conditions. In the *thermodynamic limit* of infinitely many sites the ground-state energy per site of the system can thus be computed as

$$E_G := \lim_{L \rightarrow \infty} \frac{1}{L} \min_{\Psi} \langle \Psi | H | \Psi \rangle$$

$$= \lim_{L \rightarrow \infty} \frac{1}{L} \min_{\mathcal{B}_\Psi} \sum_{k=1}^L \text{Tr}[\rho_k h_k], \quad (1)$$

where  $|\Psi\rangle$  are joint states of the many-body system and where the last minimization is performed over the sets  $\mathcal{B}_\Psi := \{\rho_1, \dots, \rho_L\}$  whose elements can be obtained as reduced density matrices of some global pure state  $|\Psi\rangle$  of the system. Specifically  $\rho_k$  is the reduced density matrix of  $|\Psi\rangle$  that is associated with the triple formed by the sites  $k-1$ ,  $k$ , and  $k+1$ . For a translational invariant Hamiltonian all the terms are equal  $h_k=h$  and Eq. (1) can be written as  $\lim_{L \rightarrow \infty} \min_{\mathcal{B}_\Psi} \text{Tr}[\bar{\rho}h]$ , with  $\bar{\rho} := \sum_k \rho_k / L$  being the average over all the triples. Therefore, without the constraint  $\rho_k \in \mathcal{B}_\Psi$  the minimization would be trivial;  $E_G$  will coincide with the ground energy level of the three-sites Hamiltonian  $h$ . Taking into account the condition  $\rho_k \in \mathcal{B}_\Psi$  is what makes the calculation of  $E_G$  a *hard* problem to solve;<sup>13</sup> it requires us to minimize the energy of  $h$  by properly embedding  $\rho_k$  in the “environment” formed by the remaining sites of the many-body system.

A solution can be found by adopting the so-called multiscale entanglement renormalization Ansatz,<sup>5</sup> which, similarly to the matrix product state decomposition,<sup>6-11</sup> assumes a specific representation of the many-body state  $|\Psi\rangle$ . In particular, according to this Ansatz the wave function of an  $L$ -sites many-body system is expressed in terms of  $O(L \log_2 L)$   $m$ -dimensional tensors of two different species (i.e., the

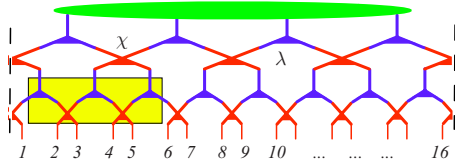


FIG. 1. (Color online) Graphical representation of a one-dimensional MERA for  $L=16$  sites. The red/gray elements correspond to the disentanglers tensors  $\chi$  while the blue/dark gray elements are the isometry tensors  $\lambda$ . The green/light gray element at the top of the MERA is a tensor which plays no role in the  $L \rightarrow \infty$  limit. The yellow/very light gray box shows the tensor compound which determines the transfer superoperator  $\Phi$  associated with the MERA (see Refs. 5 and 12 and the note 16 for details).

type- $\binom{2}{2}$  disentangler tensors  $\chi$  and type- $\binom{1}{2}$  isometry tensors  $\lambda$ ) which are connected to form the multilayer structure shown in Fig. 1 which admits efficient contraction rules (we refer the reader to Ref. 5 for details). The MERA tensor structure can be also read as a collection of transfer superoperators determined by the  $\chi$ 's and the  $\lambda$ 's tensors.<sup>5,12</sup> Such a superoperator raises the lattice description of operators to an upper level through a modified coarse-graining procedure. In the following we will restrict the minimization [Eq. (1)] to states  $|\Psi\rangle$  which can be expressed (at least approximated) by *homogeneous* MERAs, in which all the disentangler  $\chi$  and all the isometry  $\lambda$  entering the tensor network are identical.<sup>5,12</sup> Though not being such Ansatz translational invariant by itself, the thermodynamic limit  $L \rightarrow \infty$  of  $|\Psi\rangle$  can be characterized in terms of a single-transfer three-site superoperator—the QuMERA map  $\Phi$ , which performs the desired average.<sup>12,14</sup> This is the convex combination  $\Phi = (\Phi_R + \Phi_L)/2$  of the channels  $\Phi_R$  and  $\Phi_L$  whose operator sum decompositions<sup>15</sup> expressed in the computational basis are obtained by properly concatenating two copies of  $\chi$  and three copies of  $\lambda$ .<sup>16</sup> In this framework the average reduced density matrix  $\bar{\rho}$  of a neighboring triple of  $|\Psi\rangle$  can now be computed as the (unique) eigenvector  $\bar{\rho}^*$  of the QuMERA map  $\Phi$  associated with the unitary eigenvalue,<sup>12</sup> i.e.,

$$\Phi(\bar{\rho}^*) = \bar{\rho}^*. \quad (2)$$

This means that Eq. (1) can now be expressed as

$$E_G = \min_{\Phi} \text{Tr}[\bar{\rho}^* h], \quad (3)$$

where the minimization is performed over the set of all possible QuMERA channels  $\Phi$ —the equivalence being guaranteed by the stationary condition (2). The performed average is thought to converge to the single  $\rho_k$  with increasing bond dimensions of the tensors.

Equation (3) achieves two fundamental goals: (1) it allows us to directly address the thermodynamic limit  $L \rightarrow \infty$  and (2) it guarantees the possibility of reconstructing a many-body joint state  $|\Psi\rangle$  associated with the three-sites local-density operator  $\bar{\rho}^*$  (this is the MERA state corresponding to the QuMERA channel  $\Phi$ ).

The problem of finding the ground-state properties is thus reformulated in terms of the minimization of the quantity [Eq. (3)] with the additional constraint [Eq. (2)]. This reformulation allows us to compute the thermodynamic ground-

state energy employing a number of minimization steps which *do not depend* upon the system size (the limit  $L \rightarrow \infty$  being already included in the QuMERA description). In addition, once the transfer superoperator has been found via minimization, the long-range properties (critical exponents) can be easily computed in terms of secondary eigenvalues of the map itself, as shown in Ref. 12. Indeed the rescaling of the operators by the same factor through each tensor layer and the logarithmic number of layers gives rise to power-law decay of correlations,<sup>5</sup> i.e., the definition itself of scale invariance. The implementation of this algorithm, explained in the following, and the demonstration of the achievable results constitute the main result of this paper.

For the sake of self-consistency, we briefly recall here the main steps behind the calculation of the critical exponents discussed in Ref. 12 focusing on the two-point correlation functions, as the generalization is straightforward. Consider then two observables  $\Theta_k$  and  $\Theta_{k'}$  acting on the triples of sites  $k-1, k, k+1$  and  $k'-1, k', k'+1$ , respectively, (single-sites observables are trivially included as a special case). The resulting expectation values can then be written as a reiterated application of the QuMERA map on the triples subspaces, i.e.,

$$\begin{aligned} \langle \Theta_k \Theta_{k'} \rangle &= \text{Tr}[(\Phi^{\bar{\ell}} \otimes \Phi^{\bar{\ell}})(\rho_{kk'}^{(\bar{\ell})})(\Theta_k \otimes \Theta_{k'})] \\ &= \text{Tr}[\rho_{kk'}^{(\bar{\ell})}(\tilde{\Phi}^{\bar{\ell}} \otimes \tilde{\Phi}^{\bar{\ell}})(\Theta_k \otimes \Theta_{k'})], \end{aligned} \quad (4)$$

where  $\Phi$  is the QuMERA map,  $\bar{\ell} = \text{int}[\log_2(k-k')] - 1$  is the MERA level at which the *causal cones*<sup>9</sup> associated with  $k$  and  $k'$  intercept, and  $\rho_{kk'}^{(\bar{\ell})}$  is a  $6m$ -dits state associated with the overlying layers of the MERA (the explicit expression plays a marginal role in the calculation). The dual map  $\tilde{\Phi}$  is defined as the ascending one for physical operators. As the distance  $|k-k'|$  among the triples increases Eq. (4) can be simplified by exploiting the spectral property of  $\Phi, \tilde{\Phi}$ . In particular, the correlation function  $\Delta_{kk'} \equiv \langle \Theta_k \Theta_{k'} \rangle - \langle \Theta_k \rangle \langle \Theta_{k'} \rangle$  yields

$$|\Delta_{kk'}| \simeq c|k-k'|^{-\eta} \quad (5)$$

with  $\eta = -2 \log_2 |\kappa|$  with  $\kappa$  being the eigenvalue of  $\tilde{\Phi}$  with largest eigenvalue whose associated eigenoperator contributes in the expansion of Eq. (4) and  $c$  is a constant.<sup>12</sup>

In order to solve the constrained minimization problem, we proceed with an iterative procedure starting from an initial guess  $\Phi_0$  and  $\rho_0^*$  for the QuMERA channel  $\Phi$  and its associated eigenvector  $\rho^*$ . Specifically, the  $\chi$  and the  $\lambda$  tensors entering in the definition of the transfer superoperator  $\Phi$  are given by an initial guess  $\chi_0$  and  $\lambda_0$  which we optimize by varying each of them one at the time. For instance, one can start from the tensors  $\chi$  by solving the problem  $\min_{\chi} \{\text{Tr}[\Phi^{[\chi, \lambda_0]}(\rho_0^*) h]\}$  while keeping fix the initial guess for  $\lambda_0$  and  $\rho_0^*$  (here  $\Phi^{[\chi, \lambda_0]}$  is the channel associated with the MERA obtained by replacing the  $\chi_0$  of the initial guess  $\Phi_0 = \Phi^{[\chi_0, \lambda_0]}$  with some generic  $\chi$ ). Once found the optimal value  $\chi_1$  of  $\chi$  we replaced it into  $\Phi_0$  and start optimizing with respect to  $\lambda$  by solving the problem

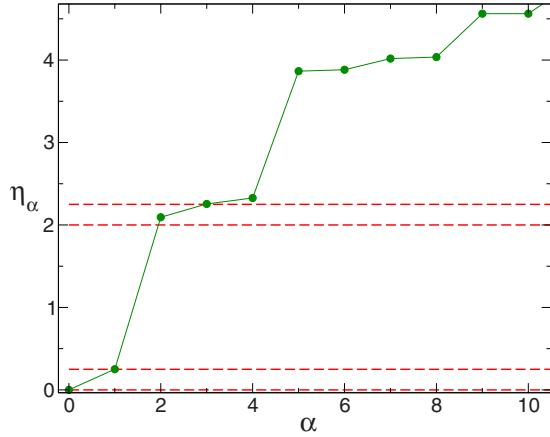


FIG. 2. (Color online) Modulus of the computed critical exponents  $\eta_\alpha$  for the Ising model for  $b=1$ ,  $\gamma=1$  (green circle). The dashed red lines correspond to the theoretical values—see Table I.

$\min_\lambda \{\text{Tr}[\Phi^{[\chi_1, \lambda]}(\rho_0^*)h]\}$ , where again  $\rho_0^*$  is kept equal to the initial guess. Possible strategies to solve such minimizations have been presented in Ref. 17 where *unconstrained quadratic optimization* have been considered. This approach is not longer applicable in our case where, for instance, the homogeneity constraint adopted to deal with the translational invariance of the system, forces all the  $\chi$ 's entering in  $\text{Tr}[\Phi^{[\chi, \lambda_0]}(\rho_0^*)h]$  to be identical while transforming the minimization in a nonquadratic optimization problem. To cope with this we approach the optimization by computing at each step the linearized gradient on a basis for the tensors belonging to the MERA while alternating moving from the  $\chi$ 's to the  $\lambda$ 's. Once the gradient is computed we move the tensor in a random direction whose signs in a given basis (going forward or backward along a given direction) are defined by the gradient's ones as in Ref. 18. Once the optimization of the  $\chi$  and the  $\lambda$  have been performed and a new QuMERA channel  $\Phi_1 = \Phi^{[\chi_1, \lambda_1]}$  is defined, the stability constraint [Eq. (2)] has to be fulfilled. Hence, we replace  $\rho_0^*$  with a new trial  $\rho_1^*$  defined as the solution of the eigenproblem  $\Phi_1(\rho_1^*) = \rho_1^*$ , which, due to  $\rho_0^*$  being a “good guess” for the new eigenvector, can be addressed by using some smart eigenproblem solvers as the Lanczos or Davidson algorithms (the results presented in the next sections are obtained using the latter). We can then proceed again in optimizing another tensor belonging to the transfer superoperator up to the desired convergence. Notice that this procedure is not guaranteed to converge to the optimal minimum, however, in general, gives good results.

The model we consider to test the above described method is defined through the (dimensionless) Hamiltonian

$$H = -\frac{1}{2} \sum_j [(1 + \gamma)\sigma_j^x \sigma_{j+1}^x + (1 - \gamma)\sigma_j^y \sigma_{j+1}^y + \Delta \sigma_j^z \sigma_{j+1}^z + 2b\sigma_j^z], \quad (6)$$

where  $\sigma_i^\alpha$  ( $\alpha=x, y, z$ ) are the Pauli matrices of the  $i$ th spin. The constants  $\Delta$ ,  $\gamma$ , and  $b$ , respectively, characterize the anisotropy in the  $z$  direction, in the  $XY$  plane and an external magnetic field. Hamiltonian (6) has a very rich structure. We

TABLE I. Theoretical and computed critical exponents for the Ising model and the relative error  $\varepsilon$  for  $m=4$ .

$\alpha$	$\eta_\alpha^{\text{th}}$	$\eta_\alpha^{\text{num}}$	$\varepsilon$ (%)
$x$	0.25	0.2509	0.36
$y$	2.25	2.2544	0.19
$z$	2	2.0939	4.48

consider two cases: (i) the Ising model in a transverse field. Here one has  $\Delta=0$  and  $\gamma=1$ . The model has a critical point at  $|b_c|=1$ ; (ii) the XXZ anisotropic Heisenberg model; here one has  $b=\gamma=0$  and  $\Delta$  generic. In this case Hamiltonian (6) is critical for  $-1 \leq \Delta \leq 1$  while it has ferromagnetic or anti-ferromagnetic order for  $\Delta > 1$  or  $\Delta < -1$ , respectively. In both cases critical exponents related to the correlation functions  $\langle \sigma_k^\alpha \sigma_{k'}^\alpha \rangle - \langle \sigma_k^\alpha \rangle \langle \sigma_{k'}^\alpha \rangle \propto |k-k'|^{-\eta_\alpha}$ , are known exactly:  $\eta_z=2$ ,  $\eta_x=0.25$ , and  $\eta_y=2.25$  for the Ising model<sup>19</sup> and  $\eta_x = \eta_y = 1/\eta_z = 1 - \arccos(\Delta)/\pi$  for the XXZ model.<sup>20</sup> We will compare our numerical results against these values and show that already with moderate tensor dimensions the agreement is good.

The algorithm we developed for solving the minimization of Eq. (3) requires to store order of  $O(m^6)$  tensors with  $m$  being the dimension of the indexes of the  $\chi$ 's and  $\lambda$ 's, their multiplication [ $O(m^{10})$  operations] and their diagonalization. As for the t-MERA,<sup>21</sup> this is “reasonable” up to  $m=4, 6$ .

We first concentrate on the Ising model, where we have obtained an energy convergence to the exact energy per site of the ground state at the thermodynamic limit on the order of  $\delta E \sim 10^{-4}$ . In Fig. 2 we report (in increasing order) the critical exponents found by means of the minimization strategy we presented in the last section from the eigenvalues  $\kappa_\alpha$  of the QuMERA map  $\Phi$ , i.e.,  $\eta_\alpha = -2 \log_2 |\kappa_\alpha^{\text{th}}|$ . As discussed in Ref. 12, from general properties of quantum channels we expect the first eigenvalue ( $\kappa_0=1$ ) and the correspondent exponent ( $\eta_0=0$ ) to be nondegenerate. The subsequent exponents instead express the critical exponents of the system as

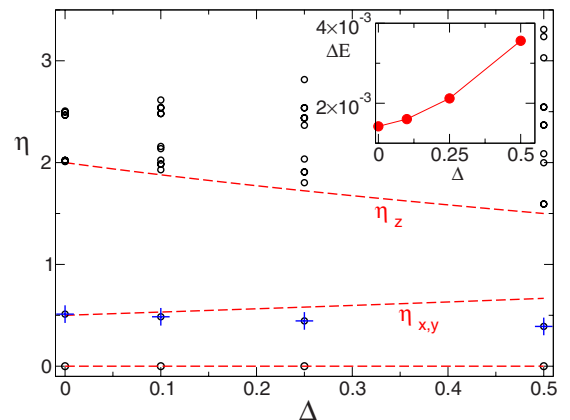


FIG. 3. (Color online) Critical exponents and of the XXZ model for various values of  $\Delta$  for  $m=4$  (black circles and blue crosses). The red dashed lines reports the theoretical values. The inset shows the correspondent error on the ground energy per site.

in Eq. (5). The dashed red lines of the figure report the theoretical expectations of the critical exponents. The result is good, the first one is exact up to the machine precision while the others have numerical errors as shown in Table I.

The results obtained for the Ising model are very promising, however it is well known that the Ising model has a simple spectrum and properties due to the fact that it is equivalent to free fermions.<sup>19</sup> We then afford the study of a more complex model, the XXZ model which corresponds to interacting fermions.<sup>20</sup> In the inset of Fig. 3 we show the error with respect to the exact energy ground state at the thermodynamic limit for various values of  $\Delta$ . As expected, the error is increasing with  $\Delta$ , however it remains on the order of  $\delta E \sim 10^{-3}$ . In Fig. 3 we show the correspondent critical exponents. As it can be seen, the unital eigenvalue is always present (at almost machine precision) while the first two degenerate eigenvalues are related to the  $\eta_x, \eta_y$  critical exponents (black circle and blue crosses) with errors increas-

ing with  $\Delta$  reflecting the precision in the energy of the ground state. The third critical exponent is also detected with even a better precision than the first two.

In conclusion we have introduced an algorithm to exploit the QuMERA channel properties and find numerically the critical exponents of critical one-dimensional many-body quantum systems. We have tested the new algorithm against the analytical solutions of the Ising and XXZ model. With minor changes the same algorithm can be applied to two-dimensional critical systems. We would also like to note that recently, two related works appeared which employ a modified MERA tensor network representation (Refs. 22 and 23).

This work was in part founded by the Quantum Information research program of Centro Ennio De Giorgi of Scuola Normale Superiore. We acknowledge financial support from the EU through the IP-SCALA and IP-EUROSQIP, and from SFB/TRR21.

<sup>1</sup>N. Goldenfeld, *Lectures on Phase Transitions and the Renormalization Group* (Addison-Wesley, New York, 1992).

<sup>2</sup>J. Zinn-Justin, *Quantum Field Theory and Critical Phenomena* (Clarendon, Oxford, 2002).

<sup>3</sup>F. Verstraete and J. I. Cirac, arXiv:cond-mat/0407066 (unpublished); V. Murg, F. Verstraete, and J. I. Cirac, Phys. Rev. A **75**, 033605 (2007).

<sup>4</sup>W. Dür, L. Hartmann, M. Hein, M. Lewenstein, and H.-J. Briegel, Phys. Rev. Lett. **94**, 097203 (2005); S. Anders, M. B. Plenio, W. Dür, F. Verstraete, and H.-J. Briegel, *ibid.* **97**, 107206 (2006).

<sup>5</sup>G. Vidal, Phys. Rev. Lett. **99**, 220405 (2007); **101**, 110501 (2008).

<sup>6</sup>U. Schollwöck, Rev. Mod. Phys. **77**, 259 (2005).

<sup>7</sup>M. Fannes, B. Nachtergaele, and R. F. Werner, Lett. Math. Phys. **25**, 249 (1992).

<sup>8</sup>S. Ostlund and S. Rommer, Phys. Rev. Lett. **75**, 3537 (1995).

<sup>9</sup>G. Vidal, Phys. Rev. Lett. **91**, 147902 (2003).

<sup>10</sup>F. Verstraete, D. Porras, and J. I. Cirac, Phys. Rev. Lett. **93**, 227205 (2004).

<sup>11</sup>K. Hallberg, Adv. Phys. **55**, 477 (2006).

<sup>12</sup>V. Giovannetti, S. Montangero, and R. Fazio, Phys. Rev. Lett. **101**, 180503 (2008).

<sup>13</sup>D. Aharonov, D. Gottesman, S. Irani, and J. Kempe, Commun.

Math. Phys. **287**, 41 (2009); N. Schuch, I. Cirac, and F. Verstraete, Phys. Rev. Lett. **100**, 250501 (2008).

<sup>14</sup>V. Giovannetti, S. Montangero, M. Rizzi, and R. Fazio, Phys. Rev. A **79**, 052314 (2009).

<sup>15</sup>I. Bengtsson and K. Życzkowski, *Geometry of Quantum States* (Cambridge University Press, Cambridge, England, 2006).

<sup>16</sup>Indicating with  $\{L_r\}_r$  and  $\{R_r\}_r$  the Kraus operators of the operator sum representation of  $\Phi_L$  and  $\Phi_R$ , respectively, we can write  $[L_r]_{\ell_1, \ell_2, \ell_3}^{u_1, u_2, u_3} = [\lambda \chi \lambda \chi \lambda]_{r_1, \ell_1, \ell_2, \ell_3, r_2, r_3}^{u_1, u_2, u_3}$  and  $[R_r]_{\ell_1, \ell_2, \ell_3}^{u_1, u_2, u_3} = [\lambda \chi \lambda \chi \lambda]_{r_1, r_2, \ell_1, \ell_2, \ell_3, r_3}^{u_1, u_2, u_3}$  with  $r \equiv (r_1, r_2, r_3)$  and with the product  $\lambda \chi$  and being the tensors of elements  $[\lambda \chi]_{\ell_1, \ell_2, \ell_3}^{u_1, u_2} \equiv \sum_i \lambda_{\ell_1, i}^{u_1} \chi_{i, \ell_2, \ell_3}^{u_2}$  and  $[\chi \lambda]_{\ell_1, \ell_2, \ell_3}^{u_1, u_2} \equiv \sum_i \chi_{\ell_1, \ell_2, i}^{u_1} \lambda_{i, \ell_3}^{u_2}$ .

<sup>17</sup>G. Evenbly and G. Vidal, Phys. Rev. B **79**, 144108 (2009).

<sup>18</sup>A. W. Sandvik and G. Vidal, Phys. Rev. Lett. **99**, 220602 (2007).

<sup>19</sup>E. Lieb, T. Schultz, and D. Mattis, Ann. Phys. **16**, 407 (1961); P. Pfeuty, *ibid.* **57**, 79 (1970).

<sup>20</sup>*Quantum Magnetism*, Lecture Notes in Physics Vol. 645, edited by U. Schollwöck, J. Richter, and D. J. J. Farnell (Springer, Berlin, 2004), p. 381.

<sup>21</sup>M. Rizzi, S. Montangero, and G. Vidal, Phys. Rev. A **77**, 052328 (2008).

<sup>22</sup>R. N. C. Pfeifer, G. Evenbly, and G. Vidal Phys. Rev. A **79**, 040301(R) (2009).

<sup>23</sup>G. Evenbly and G. Vidal, Phys. Rev. Lett. **102**, 180406 (2009).